Trajectory Processes that Preserve Uniformity: A Stochastic Geometry Perspective

S. Enayati[1], H. Saeedi[1], and H. Pishro-Nik[2]
[1]Tarbiat Modares University, Tehran, Iran,
[2]University of Massachusetts, Amherst, MA, USA

***Abstract*— Stochastic geometry has been successfully applied for performance analysis of wireless networks. Performance of some emerging applications such as unmanned aircraft systems (UAS) relies heavily on unique mobility characteristics that are sometimes not fully captured by the current stochastic geometry results. This paper focuses on this issue by introducing families of trajectory processes that preserve uniformity within a cell in the framework of aerial base stations (ABS) networks. This means if the ABS move according to such trajectory processes, they will be distributed according to a binary point process (BPP) at any time snapshot. We propose two families of such processes, namely spiral and oval processes, and analytically prove our claim. We then focus on 2 special cases of such processes, namely, radial and ring processes and demonstrate their attractive properties as far as implementation is concerned.**

I. Introduction

Many current and future engineering systems are composed of a large number mobile intelligent agents. In such systems, mobile agents might move along non-deterministic paths (trajectories). An immediate example of such systems is the future generations of Unmanned Aircraft Vehicles (UAV) [1]. Such systems usually produce heterogeneous and stochastic traffic and introduction of this new paradigm has caused major concern on how to integrate UAVs into the national airspace system while avoiding possible incidents with conventional manned air traffic already in place. Nevertheless, there is currently no rigorous probabilistic theory that can effectively capture the dynamics of such systems.

In this paper, we focus on a subset of UAVs called Aerial Base Stations (ABS) which have recently received great attention [2]. Accordingly, numerous works have been published on different aspects of ABSs which have been reviewed in the extended version of this paper [3]. ABSs can be deployed statically or mobile. Nevertheless, a major advantage of ABSs compared to their terrestrial counterparts is in fact their mobility [4] which can significantly improve the user experience in terms of average fade duration (AFD). Moreover, it has been generally stated in the literature that mobile ABSs (usually with fixed wing) outperform fixed ones (usually with rotary-wing) with respect to energy consumption [5]. However, an important question is how an acceptable coverage can also be provided. Therefore, the goal here is to design trajectory processes for mobile ABSs, so that they can provide a relatively uniform and sustainable coverage over a given area. In this regard, stochastic geometry has been successfully applied for performance analysis of wireless networks. However, the analysis is usually carried out assuming networks of static terrestrial base stations and is not directly applicable to network of mobile ABSs.

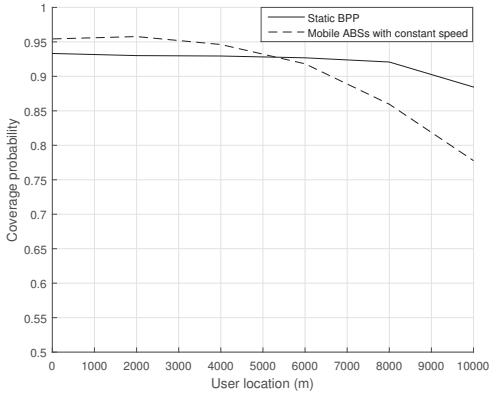

Fig. 1. Coverage probability vs. distance to origin for a cell with radius $\rho = 10$ km and 10 ABSs. For static case, ABSs are distributed according to BPP. For the mobile case, the ABSs move with constant speed of 5 m/s.

Let's assume the desired area is a cell with radius ρ. If the points (ABSs) were static, a uniform binomial point process (BPP), where points are uniformly and independently distributed across the cell, would seem to be a reasonable choice to provide a relatively uniform coverage as it is considered in the literature [6]. To address the case of mobile ABSs, we formulate the trajectory process problem in the following way: design a trajectory process involving N ABSs such that at any time $t > \tau$, the snapshot locations of the points are distributed according a uniform BPP in the cell, for some positive τ.

To see the importance of having BPP distribution at any time snapshot, in Fig. 1 for a given signal to noise ratio threshold, we have plotted the coverage probability across the cell for the static case in which the points are distributed according to BPP, with a solid curve. As can be seen, a fairly uniform coverage is achievable. Now we assume the ABSs start moving based on a trivial trajectory, for example, they move with a constant speed across the cell. The dashed curve shows the coverage in this case which does not provide an equally well user experience. The reason is that at any snap shot, the points are not distributed according to a BPP any more even though they initially were.

In this paper, we address the trajectory process problem proposed above by introducing families of trajectory processes that can preserve the uniformity at each time snapshot of the network. So far, we have been able to identify two families

978-1-5386-4780-6/18/$31.00©2018 IEEE

of such trajectory processes, referred to as *spiral* and *oval* trajectory processes.

In spiral trajectory processes, each ABS generally starts flying from the cell origin towards the cell edge according to the specs itemized in Definition 1 of the next section. An important member of this family is called the radial trajectory process in which the trajectories are in fact randomly-selected cell radii. In oval trajectory processes, each ABS moves on a closed curve, containing the cell origin within it according to the specs itemized in Definition 2 of the next section. An important member of this family is called the ring trajectory process in which the trajectories are circles with different radiuses, all centered on the cell origin.

In the extended version of this paper [3], we simulate a network based on radial and ring processes and show that they can improve AFD by two orders of magnitude while providing a uniform coverage similar to the case of static BPP. Moreover, we have proposed deterministic counterparts of the radial and ring processes and proved that they have similar statistical properties. This makes the proposed scheme even more practical and implementable.

Finally, it is important to note that application of results of this paper is not limited to ABS networks. In fact, in many other scenarios, we do prefer to have the UAVs distributed uniformly across an area. An immediate example is when we are performing a search and rescue operation using UAVs and if the uniformity is preserved, it can result in higher probability of success in the operation.

II. Stochastic trajectory processes that provide uniform coverage

A. Some basic facts

If a fixed number of points are independently and identically distributed (i.i.d) on a compact set $W \in R^d$, we say the points can be modeled as a general BPP. If these points are distributed uniformly within the same compact set, then we say the points are modeled according to a uniform BPP [7].

Now suppose that N ABSs at height H are distributed according to a BPP and start their flights following an arbitrary trajectory process, $\{\mathbf{X}_1(t), \mathbf{X}_2(t), \mathbf{X}_3(t), \cdots\}$ at times $T_1, T_2, ..., T_N$, independently chosen randomly from $(0, \tau)$ according to a given PDF (It is assumed that the trajectory curves are chosen independently from a certain probability space, and are independent from the starting times $T_1, T_2, ..., T_N$). It can be easily seen that at any arbitrary observation time of $t' \geq \tau$, the ABSs still follow a general BPP. However, if these ABSs are distributed according to uniform BPP and move according to an arbitrary trajectory, at a given time instant, the ABSs do not necessarily follow a uniform BPP model.

B. Spiral Trajectory Processes

1) General theorem: For $\underline{c} = (c_x, c_y) \in \mathbb{R}^2$, let $B(\underline{c}, \rho) = \{(x, y) \in \mathbb{R}^2 : (x-c_x)^2+(y-c_y)^2 \leq \rho^2\}$. Let also $\underline{O} = (0, 0)$. Then we state the following definition:

Definition 1. *Let $\underline{X}(s) : [0, 1] \mapsto B(\underline{O}, \rho)$ be twice differentiable curves, $\underline{X}(s) = (x(s), y(s))$, with the following properties:*

1) $\underline{X}(0) = \underline{O}$, $x(1)^2 + y(1)^2 = \rho^2$;
2) $r(s) \triangleq \sqrt{x(s)^2 + y(s)^2}$ *is a strictly increasing function of s for all $s \in [0, 1]$.*

Now for any $\tau > 0$, define the mappings $h : [0, 1] \mapsto [0, \tau]$ as $h(s) = \frac{\tau r(s)^2}{\rho^2}$. Suppose that N aerial vehicles start their flights at times $T_1, T_2, ..., T_N$, independently chosen uniformly from $(0, \tau)$. For $k\tau + T_i \leq t \leq (k + 1)\tau + T_i$, we define the ***spiral trajectories*** *$\tilde{X}_i(t) = (\tilde{x}_i(t), \tilde{y}_i(t))$ for the i'th vehicle as Eq. (1) on the next page. In (1), ROT_{Θ_i} is the rotation around the origin by Θ_i degrees where $\Theta_i \sim U(0, 2\pi)$ are chosen independently when the vehicle starts its departure from the origin.*

In order to have a better insight of the curves satisfying Properties 1 and 2, we provide a family of general curves here. Assume that

$$\underline{X}(s) = [\rho s^k cos(\zeta s), \rho s^k sin(\zeta s)], \quad s \in [0, 1], \tag{2}$$

where depending on the values of ρ, k and ζ, different curves can be generated. For example by setting $\rho = 5$, $k = 2$ and $\zeta = 2\pi$ we obtain curves in Fig. 2 where $X_2(s) = -X_1(s)$. Now we are ready to state the following theorem:

Theorem 1. *For all $t > \tau$, the instantaneous locations of the aerial vehicles on the spiral trajectory, i.e., $\tilde{X}_i(t) = (\tilde{x}_i(t), \tilde{y}_i(t))$, form a uniform BPP in $B(\underline{O}, \rho)$.*

Before providing the proof, we present the following lemma which will be used later in the proof procedure.

Lemma 1. *Consider a periodic function $g : \mathbb{R} \mapsto [0, \infty)$, where $g(t + \tau) = g(t), \forall t \in \mathbb{R}$. $F_{R(t)}(r)$, the CDF of the randomly shifted process $R(t) \triangleq g(t - T), T \sim U(0, \tau)$, is obtained by*

$$F_{R(t)}(r) = \frac{|\mathcal{A}|}{\tau}, \tag{3}$$

where $|.|$ is the Lebesgue measure of $\mathcal{A}$ defined as $\mathcal{A} = \{\alpha \in [0, \tau] |\ g(\alpha) \leq r\}$.

Proof.

$$\begin{aligned} F_{R(t)}(r) &= \int_0^\tau \Pr\left(g(t - T) \leq r | T = \alpha\right) f_T(\alpha) d\alpha \\ &= \frac{1}{\tau} \int_0^\tau 1_{\{g(t-\alpha) \leq r\}} d\alpha = \frac{|\mathcal{A}|}{\tau}, \end{aligned} \tag{4}$$

where $\mathcal{A}$ is defined as the region in which $g(\alpha) \leq r$ during one period, i.e., $\mathcal{A} = \{\alpha \in [0, \tau] | g(\alpha) \leq r\}$. □

Corollary 1. If we have $g(2\tau - t) = g(t), t \in (0, \tau)$, and $R(t) \triangleq g(t - T), T \sim U(0, \tau)$, we get a similar distribution since $g(t)$ is symmetric with respect to τ.

We now provide the proof for Theorem 1.

Proof. For the proof of Theorem 1, we first need to show that for $t \geq \tau$, the location of vehicles are independent. This is intuitive since $\Theta_i \sim U(0, 2\pi)$ and $T_i \sim U(0, \tau)$ both have been chosen independently. Second, we have to show that the locations are uniformly distributed in $B(\underline{O}, \rho)$. To do so, we note that since $\Theta_i \sim U(0, 2\pi)$, the phase of an arbitrary point on the curve is uniformly distributed between 0 and 2π, i.e.,

$$(\tilde{x}_i(t), \tilde{y}_i(t)) = \begin{cases} ROT_{\Theta_i}\Big(x_i(h_i^{-1}(t-k\tau-T_i)), y_i(h_i^{-1}(t-k\tau-T_i))\Big), & k \text{ even} \\ ROT_{\Theta_i}\Big(x_i(h_i^{-1}((k+1)\tau+T_i-t)), y_i(h_i^{-1}((k+1)\tau+T_i-t))\Big), & k \text{ odd}, \end{cases} \tag{1}$$

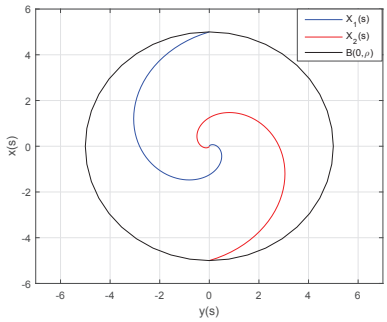

Fig. 2. Typical curves from the spiral trajectory process with $\rho = 5$, $k = 2$ and $\zeta = 2\pi$.

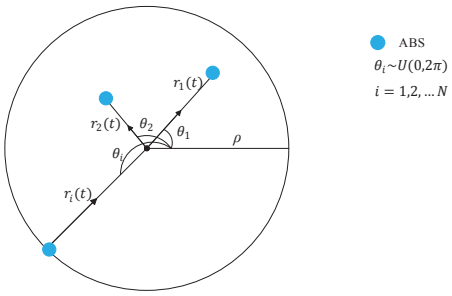

Fig. 3. An illustration of flying ABSs according to a radial trajectory process

$\angle\tilde{X}_i(t) \sim U(0, 2\pi)$. It only remains to show that the CDF of the distance between the origin and an arbitrary point on the curve, i.e., $\|\tilde{X}_i(t)\|$, is equal to the distribution corresponding to uniform BPP within $B(\underline{O}, \rho)$. For notational simplicity, we drop index i in the rest of the proof. Let

$$u(t) \triangleq \begin{cases} \|X(h^{-1}(t))\| & 0 \le t \le \tau \\ \|X(h^{-1}(2\tau - t))\| & \tau \le t \le 2\tau \end{cases}. \tag{5}$$

We provide the proof for the case of $0 \le t \le \tau$, the for the case of $\tau \le t \le 2\tau$ is similar. According to (5) and Property 2 in Definition 1, we understand that

$$u(t) = \|X(h^{-1}(t))\| = r(h^{-1}(t)). \tag{6}$$

Also, since the random rotation of $X(t)$ will not affect its absolute value, we have $\|\tilde{X}(t)\| = u(t-T)$ where $\tilde{X}(t)$ is the randomly rotated and shifted version of $X(t)$ defined in Eq. (1). Now using Lemma (1), we obtain $F_{\|\tilde{X}\|}$ as below

$$F_{\|\tilde{X}\|} = \frac{1}{\tau}|\{0 \le \alpha \le \tau : u(\alpha) \le r\}|$$

$$= \frac{1}{\tau}|\{0 \le \alpha \le \tau : \|X(h^{-1}(\alpha))\| \le r\}|. \tag{7}$$

Again, according to Property 2, since $r(s)^2$ is strictly increasing, $h(s) = \frac{\tau r(s)^2}{\rho^2}$ is also strictly increasing and hence, there exists an $\alpha_{\max}$ such that

$$\|X(h^{-1}(\alpha_{\max}))\| \le r. \tag{8}$$

Therefore, $F_{\|\tilde{X}\|} = \frac{|[0,\alpha_{\max}]|}{\tau} = \frac{\alpha_{\max}}{\tau}$. Now suppose there exists an arbitrary $0 \le \alpha^* \le \tau$ such that $\alpha^* = \frac{\tau r^2}{\rho^2}$. This means there exists a $s^* \in [0, 1]$ such that $\alpha^* = h(s^*) = \frac{\tau r^{*2}}{\rho^2}$, which means $r^* = r(h^{-1}(\alpha^*)) = r$. Therefore, we have $h^{-1}(\alpha^*) = h^{-1}(\alpha_{\max})$, according to (8). By this, we can uniquely obtain $\alpha^* = \alpha_{\max}$, since h is monotonic. Finally, the CDF can be written as

$$F_{\|\tilde{X}\|} = \frac{|\{0 \le \alpha \le \alpha_{\max}\}|}{\tau} = \frac{r^2}{\rho^2}, \tag{9}$$

which is the same as the CDF corresponding to a BPP within $B(\underline{O}, \rho)$. This completes the proof. □

The family of curves introduced by this theorem is quite diverse. In the next subsection we focus on one of the simple processes of this family called radial trajectory process.

2) Radial Trajectory Process: A sample radial trajectory process is shown in Fig. 3. It can be obtained by setting $k = 1$ and $\zeta = 0$ in Eq. (2). We assume that N ABSs start to take off from the cell center at random moments $T_1, T_2, ..., T_N \in (0, \tau)$ where τ is the initialization time in which all N ABSs start to take off. $T_1, T_2, ..., T_N$ are independently chosen uniformly from $(0, \tau)$. Each ABS first flies to a predetermined altitude of H and then chooses a random angle $\Theta_i \in (0, 2\pi)$ uniformly and flies in a straight line towards the cell edge where its distance to origin at time t is shown by the random variable $R(t)$. When an ABS reaches the cell edge, it returns to the origin on the same angle to complete the first cycle and this action repeats continuously. For each half cycle $k\tau + T_i \le t \le (k+1)\tau + T_i$, $R(t)$ has to satisfy the following formulation:

$$R_i(t) = \begin{cases} \rho\sqrt{\frac{t-T_i-k\tau}{\tau}}, & k \text{ even} \\ \rho\sqrt{\frac{(k+1)\tau+T_i-t}{\tau}} & k \text{ odd}. \end{cases} \tag{10}$$

Note that with this definition, we have $R(k\tau) = 0$ if k is even and $R(k\tau) = \rho$ otherwise. In other words, τ is the time it takes for an ABS to go from center to the edge. It is worth mentioning that during the initial take off phase, it takes a while for each ABS to get to the altitude H but we assume this time is negligible compared to τ. By the description above, one can understand that after the time τ, we have N ABSs flying at the altitude of H.

A very interesting point in radial trajectory process is the behaviour of the ABS velocity which can be obtained by taking derivative of (10):

$$V_i(t) = \begin{cases} \frac{\rho}{\sqrt{\tau(t-T_i-k\tau)}}, & k \text{ even} \\ -\frac{\rho}{\sqrt{\tau((k+1)\tau+T_i-t)}}, & k \text{ odd} \end{cases}. \quad (11)$$

Eq. (11) demonstrates that as t increases (i.e., ABS is at larger distance from the center), its velocity decreases which means that it spends longer time flying at the larger distances to provide a uniform coverage.

C. Oval Trajectory Processes

1) General theorem:

Definition 2. *For any given $a, b \in \mathbb{R}^+$, where $0 \le a \le b \le \rho$, let $\underline{X}^{a,b}(s) : [0,1] \mapsto B(\underline{O}, \rho)$ be twice differentiable curves, $\underline{X}^{a,b}(s) = (x_1^{a,b}(s), x_2^{a,b}(s))$, with the following properties:*

1) *$\underline{X}^{a,b}(0) = (0, a)$, $\underline{X}^{a,b}(1) = (b, 0)$;*
2) *$r^{a,b}(s) \triangleq \|\underline{X}^{a,b}(s)\| = \sqrt{x_1^{a,b}(s)^2 + x_2^{a,b}(s)^2}$ is a non-decreasing function of s for all $s \in [0,1]$.*

Now, for any $\tau > 0$, define the mappings $h_{a,b} : [0,1] \mapsto [0, \frac{\tau}{4}]$ as

$$h^{a,b}(s) = \frac{\tau(r^{a,b}(s) - a)}{4(b-a)}. \quad (12)$$

In addition, for $i \in \{1, 2, \cdots, N\}$, assume that random variables (A_i, B_i) are chosen independently according a two-dimensional probability distribution that satisfies $P(0 \le A_i \le B_i \le \rho) = 1$ and

$$\mathbb{E}_{A_i,B_i}\left[\frac{1_{(A_i \le r \le B_i)}}{B_i - A_i}\right] = \frac{2r}{\rho^2} \quad \text{for all } r \in [0, \rho]. \quad (13)$$

*We define the corresponding **oval trajectories** $\underline{Z}^{a,b}(t) : [0,\tau] \mapsto B(\underline{O}, \rho)$ as in Equations (14) and (15) in the next page, for $0 \le t \le \frac{\tau}{2}$ and $\frac{\tau}{2} \le t \le \tau$, respectively: Now for any ABS i, we set $a = A_i$ and $b = B_i$ to generate $Z_i^{a,b}(t)$. The **extended oval trajectories**, $\underline{\tilde{Z}}^{a,b}(t) = (\tilde{z}_1^{a,b}(t), \tilde{z}_2^{a,b}(t)) : \mathbb{R}^+ \mapsto B(\underline{O}, \rho)$, are defined by periodically extending $\underline{Z}^{a,b}(t)$ outside of $[0,\tau]$ such that*

$$\underline{\tilde{Z}}^{a,b}(t+\tau) = \underline{\tilde{Z}}^{a,b}(t), \quad \text{for } t \in \mathbb{R}^+.$$

*Suppose that N aerial vehicles start their flights at times $T_1, T_2, ..., T_N$, independently chosen uniformly from $(0,\tau)$. Let also $\underline{W}_i^{A_i,B_i}(t)$ be the corresponding **delayed extended oval trajectories** according to T_i's, i.e., for $t \in [T_i, \infty]$*

$$\underline{W}^{A_i,B_i}(t) = \underline{\tilde{Z}}^{A_i,B_i}(t - T_i).$$

*Moreover, for $t > \tau$, we define the **rotated delayed extended oval trajectories**, $\underline{\tilde{V}}_i(t) = (\tilde{v}_i(t), \tilde{v}_i(t))$ of the i'th vehicle*

$$(\tilde{v}_i(t), \tilde{v}_i(t)) = ROT_{\Theta_i}\left(\underline{W}^{A_i,B_i}(t)\right), \quad (16)$$

where ROT_{Θ_i} is the rotation around the origin by Θ_i degrees and $\Theta_i \sim U(0, 2\pi)$ is chosen independently from each other.

A family of curves satisfying the Properties 1 and 2 of Definition 2 can be defined in the following form

$$X(s) = [q\cos(\frac{\pi}{2}s), q\sin(\frac{\pi}{2}s)], \quad s \in [0,1], \quad (17)$$

where $q = a + (b-a)s$ and a and b are random variables with a two-dimensional PDF $f_{A,B}(a,b)$ that satisfies (13). Figure 4 shows a representation of Eq. (17).

Theorem 2. *For all $t > \tau$, the instantaneous locations of the aerial vehicles on the rotated delayed extended oval trajectory, i.e., $\underline{\tilde{V}}(t)$, form a uniform BPP in $B(\underline{O}, \rho)$.*

Before presenting the proof of Theorem 2, we state the following lemma which will be used in the main part of the proof.

Lemma 2. *Let $T \sim U(0,\tau)$. Fix $a, b \in \mathbb{R}^+$, where without loss of generality $0 \le a \le b \le \rho$ (since the case of $0 \le b \le a \le \rho$ can be considered as the rotated version of the former), and consider a delayed oval trajectory $\underline{\tilde{Z}}^{a,b}(t)$ as defined in Definition 2. For $t \in [T, \infty]$, define the delayed extended oval trajectory $\underline{W}^{a,b}(t)$ as*

$$\underline{W}^{a,b}(t) = \underline{\tilde{Z}}^{a,b}(t - T).$$

Then for any $t > \tau$, we have

$$\|\underline{W}^{a,b}(t)\| \sim U(a,b).$$

Proof. We provide the proof for $0 \le t \le \frac{\tau}{4}$. The proof is similar for other values of t. Similar to the procedure developed for the proof of Theorem 1, let $u(t) = \|\underline{\tilde{Z}}^{a,b}(h^{-1}(t))\|, 0 \le t \le \frac{\tau}{4}$ and $\|\underline{W}^{a,b}(t)\| = u(t-T)$, where T is a uniform random variable in the interval $(0,\tau)$. With these assumptions and using Lemma 1 we obtain

$$F_{\|\underline{W}^{a,b}\|} = \frac{4|\{0 \le \beta \le \frac{\tau}{4} : u(\beta) \le r\}|}{\tau}$$

$$= \frac{4|\{0 \le \beta \le \frac{\tau}{4} : \|\underline{\tilde{Z}}^{a,b}(h^{-1}(\beta))\| \le r\}|}{\tau}, \quad (18)$$

where since $h(s)$ defined in (12) is a non-decreasing function of s, we can say that there exists a $\beta_{\max}$ for which we have $\|\underline{\tilde{Z}}^{a,b}(h^{-1}(\beta_{\max}))\| \le r$. Hence, we get

$$F_{\|\underline{W}^{a,b}\|} = \frac{4|[0, \beta_{\max}]|}{\tau} = \frac{4\beta_{\max}}{\tau}. \quad (19)$$

On the other hand, let $0 \le \beta^* \le \frac{\tau}{4}, \beta^* = \frac{\tau(r-a)}{4(b-a)}$ which means there exists a $s^* \in [0,1]$ for which $\beta^* = h(s^*)$. Therefore, we have $h^{-1}(\beta^*) = h^{-1}(\beta_{\max})$ and since h is monotonic, we uniquely have $\beta^* = \beta_{\max}$. Finally, we obtain the CDF of the distance between any point on the first quarter located on the curve $\underline{W}^{a,b}(t)$ and the origin as below

$$F_{\|\underline{W}^{a,b}\|} = \frac{4|\{0 \le \beta \le \beta_{\max}\}|}{\tau} = \frac{4\beta_{\max}}{\tau} = \frac{r-a}{b-a}, \quad (20)$$

which is the CDF of a random variable distributed uniformly between a and b. □

Using Lemma 2, we now are able to provide the proof of the Theorem 2.

Proof. Similar to the case of Theorem 1, since $\Theta_i \in (0, 2\pi)$ and $T_i \in (0,\tau)$ are each chosen independently, we conclude that the points on the curves are independent. Now we can obtain the distribution of distances of the points on the rotated

$$\underline{Z}^{a,b}(t) = (z_1^{a,b}(t), z_2^{a,b}(t)) = \begin{cases} \left(x_1^{a,b}(h_i^{-1}(t)), x_2^{a,b}(h_i^{-1}(t))\right), & \text{for } 0 \le t \le \frac{\tau}{4} \\ \left(-x_1^{a,b}(h_i^{-1}(\frac{\tau}{2}-t)), x_2^{a,b}(h_i^{-1}(\frac{\tau}{2}-t))\right), & \text{for } \frac{\tau}{4} \le t \le \frac{\tau}{2}, \end{cases} \tag{14}$$

$$\underline{Z}^{a,b}(t) = (z_1^{a,b}(t), z_2^{a,b}(t)) = \begin{cases} \left(-x_1^{a,b}(h_i^{-1}(t-\frac{\tau}{2})), -x_2^{a,b}(h_i^{-1}(t-\frac{\tau}{2}))\right), & \text{for } \frac{\tau}{2} \le t \le \frac{3\tau}{4} \\ \left(x_1^{a,b}(h_i^{-1}(\tau-t)), -x_2^{a,b}(h_i^{-1}(\tau-t))\right), & \text{for } \frac{3\tau}{4} \le t \le \tau. \end{cases} \tag{15}$$

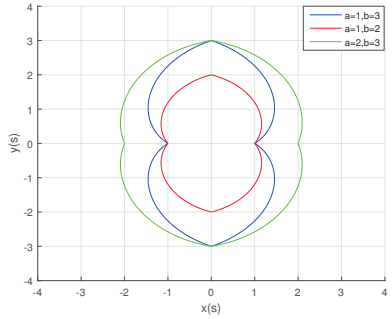

Fig. 4. Typical curves from the oval trajectory process

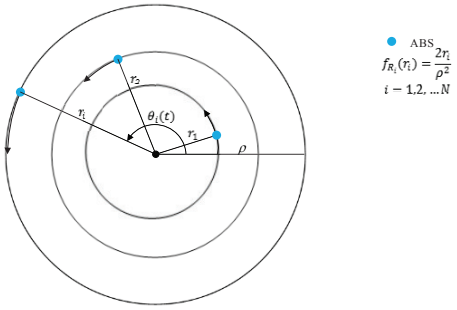

Fig. 5. An illustration of flying ABSs according to a ring trajectory process

delayed extended oval trajectory $\underline{\tilde{V}}_i(t)$ for $t \ge \tau$, $f_{\|\underline{\tilde{V}}\|}(r)$ as below

$$f_{\|\underline{\tilde{V}}\|}(r) \overset{(a)}{=} \int_a \int_b f_{\|\underline{\tilde{V}}\||A,B}(r|a,b) f_{A,B}(a,b) da db$$

$$= \mathbb{E}_{A,B}[f_{\|\underline{\tilde{V}}\||A,B}(r|a,b)] \overset{(b)}{=} \mathbb{E}_{A,B}\left[\frac{\mathbb{1}_{A\le r\le B}}{B-A}\right], \tag{21}$$

where (a) results from the law of total probability and (b) comes from Lemma 2 where we showed that given a and b, the distribution of $\|\underline{W}^{a,b}(t)\|$ is uniform in the interval (a,b). Finally, according to (13), the last statement in (21) is equal to $\frac{2r}{\rho^2}$ and so we have $f_{\|\underline{\tilde{V}}\|}(r) = \frac{2r}{\rho^2}$ which completes the proof. □

2) Ring Trajectory Process: A special case of the oval process can be obtained by assuming B_i to be a random variable with $f_{B_i}(b) = \frac{2b}{\rho^2}$ and $A_i = B_i - \epsilon$ with probability 1. With $a = b = B_i$ which results in $q = B_i$ in (17), this trajectory which is henceforth called the *ring process*, represents a circle with radius B_i on which an ABS i turns around the center with a constant speed of $v_{i,\text{ring}} = \frac{2\pi B_i}{\tau}$. Such a constant speed is a major practical advantage over other members of the oval trajectory family as well as the spiral trajectory. Now we have to investigate if (13) holds:

$$\mathbb{E}_{A_i,B_i}\left[\frac{\mathbb{1}_{A_i\le r\le B_i}}{B_i - A_i}\right] = \frac{1}{\epsilon}\Pr\left(B_i - \epsilon \le r \le B_i\right)$$

$$= \frac{1}{\epsilon}\int_r^{r+\epsilon} f_{B_i}(b) db = \frac{2r+\epsilon}{\rho^2}. \tag{22}$$

As $\epsilon \to 0$, the expectation tends to $\frac{2r}{\rho^2}$, proving the assertion.

III. Conclusion

In this paper, we designed stochastic trajectory processes involving N points (ABSs) such that at any snapshot, the locations of the points are distributed according a uniform BPP in the cell. For a network of ABSs, this guarantees a uniform coverage for the users across the cell. We introduced two families of such processes, namely spiral and oval processes and analytically proved the uniformity. Then we considered two specials cases of the proposed families, radial and ring processes. These two trajectory processes can be conveniently implemented and are thus of practical interest.

References

[1] L. Gupta, R. Jain, and G. Vaszkun, "Survey of important issues in UAV communication networks," *IEEE Communications Surveys & Tutorials*, vol. 18, no. 2, pp. 1123–1152, Secondquarter, 2016.

[2] S. Hayat, E. Yanmaz, and R. Muzaffar, "Survey on unmanned aerial vehicle networks for civil applications: a communications viewpoint," *IEEE Communications Surveys & Tutorials*, vol. 18, no. 4, pp. 2624–2661, Fourthquarter 2016.

[3] S. Enayati, H. Saeedi, and H. Pishro-Nik, "Mobile aerial base station networks: Stochastic geometry analysis and design perspective," *Submitted to IEEE Journal of Selected Areas in Communications*. [Online]. Available: www.ecs.umass.edu/ece/pishro/Papers/ABS.pdf.

[4] S. Chandrasekharan, K. Gomez, A. Al-Hourani, S. Kandeepan, T. Rasheed, L. Goratti, L. Reynaud, D. Grace, I. Bucaille, T. Wirth *et al.*, "Designing and implementing future aerial communication networks," *IEEE Communications Magazine*, vol. 54, no. 5, pp. 26–34, May 2016.

[5] F. Ono, H. Ochiai, and R. Miura, "A wireless relay network based on unmanned aircraft system with rate optimization," *IEEE Transactions on Wireless Communications*, vol. 15, no. 11, pp. 7699–7708, Nov 2016.

[6] V. V. Chetlur and H. S. Dhillon, "Downlink coverage analysis for a finite 3D wireless network of unmanned aerial vehicles," *IEEE Transactions on Communications*, vol. 65, no. 10, pp. 4543–4558, Oct. 2017.

[7] M. Haenggi, *Stochastic Geometry for Wireless Networks*. Cambridge University Press, 2012.